DOI: 10.13009/EUCASS2019-630

8th European conference for aeronautics and space sciences (EUCASS)

IXV Mission Analysis Post Flight

Davide Bonetti, Gabriele De Zaiacomo*, Gonzalo Blanco Arnao*, Irene Pontijas Fuentes*, Antonio Pagano**

**Deimos Space S.L.U. davide.bonetti@deimos-space.com, Ronda de Poniente 19, 28760 Tres Cantos, Spain*

Abstract

The ESA Intermediate eXperimental Vehicle (IXV) developed and tested in flight key technologies and critical systems for an autonomous and controlled re-entry from low Earth orbit. The successful flight of the IXV on February, 11th, 2015 marked a new milestone in European re-entry, and allowed to tackle the basic European needs for re-entry from Low Earth Orbit (LEO) and to consolidate the knowledge necessary for the development of any future European reusable re-entry system while allowing guaranteeing risk limitation. IXV is a lifting body vehicle that performed a suborbital mission targeting typical LEO return conditions, re-entered the atmosphere making use of two movable flaps for aerodynamic control, and performed a descent under a multi-stage parachute to safely splashdown in the Pacific Ocean. The successful IXV mission allowed to recover all the in-flight data and its use for a post-flight analysis.
IXV represented an opportunity to increase the technology readiness level (TRL) not only of technologies but also of design methodologies and tools. Disciplines like the Mission Analysis and Flight Mechanics, for which DEIMOS Space has been the responsible, have followed the vehicle from the conceptual design up to post flight analyses.
This paper presents the results of the IXV post flight Mission Analysis. Data collected from the telemetry of the successful flight have been used for the numerical reconstruction of the IXV trajectory, for the flight validation of the mission design and flight predictions and for the derivation of lessons learned, which have been readily injected in the ongoing Space Rider program.

1. Introduction

The Intermediate eXperimental Vehicle (IXV) program achieved a major success for the European space industry and the European Space Agency (ESA), when the IXV was launched by a VEGA rocket at 13:40 UTC on February the 11th, 2015, and returned to Earth with a flawless re-entry. The vehicle performed a splashdown in the Pacific Ocean about 97 minutes after lift-off, and was successfully recovered. The IXV was an ESA re-entry lifting body demonstrator built to verify in-flight the performance of critical re-entry technologies during the re-entry phase ([1],[2]). The IXV´s flight and recovery represent a major step forward with respect to previous European re-entry experience (e.g. the Atmospheric Re-entry Demonstrator [3]). In particular, the increased in-flight maneuverability achieved from the lifting body permitted the verification of technologies over a wider re-entry corridor, the re-entry flight from orbital speeds with the lifting body aeroshape was a first for Europe and worldwide, and the combination of thrusters and aerodynamic surfaces for control was a first for Europe.
A key part of the IXV developments and advances was the Mission Engineering [4], during which mission analysis and design were performed during the IXV program in support to the System activities since the conceptual design up to the operations. The IXV Mission and Flight Mechanics design represents an end-2-end process that involved analyses during all phases of the sub-orbital flight from the VEGA lift-off, until splashdown (see Figure 1), through the entire set of flight phases; ascent, orbital coasting, re-entry and descent. In IXV, the role of Mission Analysis and Flight Mechanics has mainly covered design (mission, vehicle configuration) and the provision of inputs to build the specification of system and subsystems. After the Critical Design Review, the role changed from design to design update and verification as well as the provision of inputs for the detailed design of different subsystems. This activity ended by the System and Qualification Acceptance Review (SQAR). During the preparation of the launch campaign the activities were related to the provision of flight predictions to support the operations, selection of on-board parameters and final go-ahead decisions in the mission control centre.
The IXV Mission Analysis was the responsibility of DEIMOS, under the supervision of Thales Alenia Space – Italy (TAS-I), the main contractor for the IXV program. The same role is now covered by DEIMOS within the Space Rider program [10], under contract with TAS-I, responsible of the Spacer Rider Re-entry Module, an operational

DOI: 10.13009/EUCASS2019-630

version of the IXV vehicle. No formal post-flight analysis for the IXV was performed, but preliminary post-flight information on the IXV mission [6][7] and the Guidance Navigation and Control (GNC) performance [8][9] are available. This paper provides further insights on the IXV in-flight performance reporting the level 1 post-flight analysis carried out as part of the Space Rider Preliminary Design activities, within the phase B2 of the Space Rider program.

The main objectives of the analyses were to evaluate the mission analysis and flight mechanics performance of the IXV mission, compare them with the pre-flight predictions, and validate the mission design process, in order to inject the lessons learned into the Spacer Rider design.

This paper summarizes the post-flight mission analysis and the validation of the Mission Engineering design process of the IXV. The IXV mission and the available flight data are discussed, and the flight reconstruction process is described. The flight mechanics performances are then presented and the flight mechanic design validated. Afterwards, the main trajectory performances are presented, and compared with the pre-flight predictions in order to validate the mission design.

Figure 1: The IXV after the successful re-entry (credits: ESA).

2. IXV Mission and Flight Data

The IXV shape and size are shown in Figure 3. The IXV is a 5 m long lifting body with a mass of about 1850 kg. Able to guarantee a lift-to-drag ratio of 0.7 in the hypersonic regime, the IXV is controlled through the combination of two body flaps mounted at the aft windward side of the vehicle and Reaction Control System (RCS) thrusters.

The IXV was launched from Kourou by the 4th flight of the VEGA launcher (Figure 2), and then injected into a suborbital trajectory after separation from the upper stage of the VEGA rocket (AVUM), see Figure 4. It then performed a ballistic coasting phase with an apogee of about 413 km, until reaching the Entry Interface Point (EIP), defined at 120 km altitude, which defines the boundary of the sensible atmosphere. RCS is the only active attitude control element during this orbital phase. The flaps were kept at a pre-defined attitude that, in case of failure, would guarantee a spinning motion that would lead to the breakup of the vehicle during an uncontrolled re-entry. A check out maneuver was planned during the orbital phase to verify the correct functioning of the flaps. The conditions at the EIP were typical of LEO return missions, with co-rotating velocities higher than 7.4 km/s. The IXV then performed a guided gliding re-entry from the EIP until reaching the conditions for the Descent and Recover System (DRS) triggering, at which time the descent phase sequence with a 3 stages parachute system is triggered. Attitude control during the re-entry phase was carried out mainly by aerodynamic means, the flaps, combined with the RCS. The supersonic chute was deployed at the DRS triggering conditions of about Mach 1.5 at an altitude of 25.5 km. The flight terminated at splashdown in the Pacific Ocean, with a flotation system maintaining IXV in conditions suitable for the recovery ship (Figure 1).

The IXV flight data of interest for the Post-Flight Mission Analysis are the navigation solution (in terms of position, velocity and attitude in different reference frames), the commanded flaps' deflection (from which the commanded elevator and aileron deflections are computed), the derived Inertial Measurement Unit (IMU) measurements (accelerations and angular rates), the GPS position-velocity-time (PVT) solution, and several GNC and on-board software (OBSW) commands. It is remarked that no direct measurement of the actual flaps' deflection was performed, and only the commanded values are directly available. Reconstruction of the flaps' deflection through direct and indirect methods was performed.

In addition to the IXV telemetry data, additional information, not available from onboard sensors, is taken from the design results. In particular:

- the MCI (Mass, CoG and Inertia) is taken from the pre-flight measurements made available for the flight predictions activities, as well as the IMU position and orientation,
- The aerodynamic and environmental models are the reference models used for the design qualification.
- Initial conditions are consistent with VEGA initial position and velocity at launch pad at lift-off.

After an initial assessment of the data, including synchronization and filtering, these flight data have been used to reconstruct the IXV trajectory and analyze the performance of the IXV flight.

The pre-flight results used for comparison are the flight prediction results obtained by the DEIMOS Space analyses performed during the phase E of the IXV program [4].

DOI: 10.13009/EUCASS2019-630

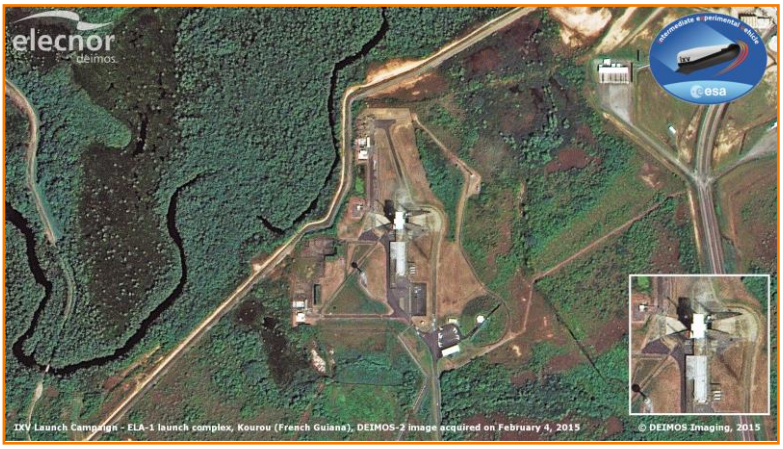

Figure 2: VEGA on the launch pad getting ready for the VV04 mission.

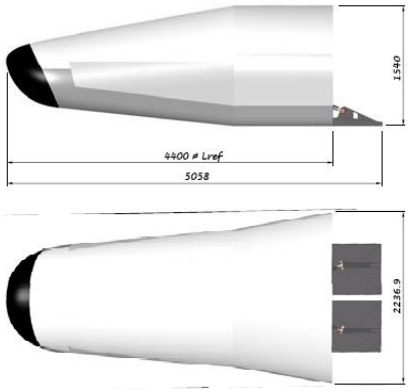

Figure 3: The IXV aeroshape (credits: TAS).

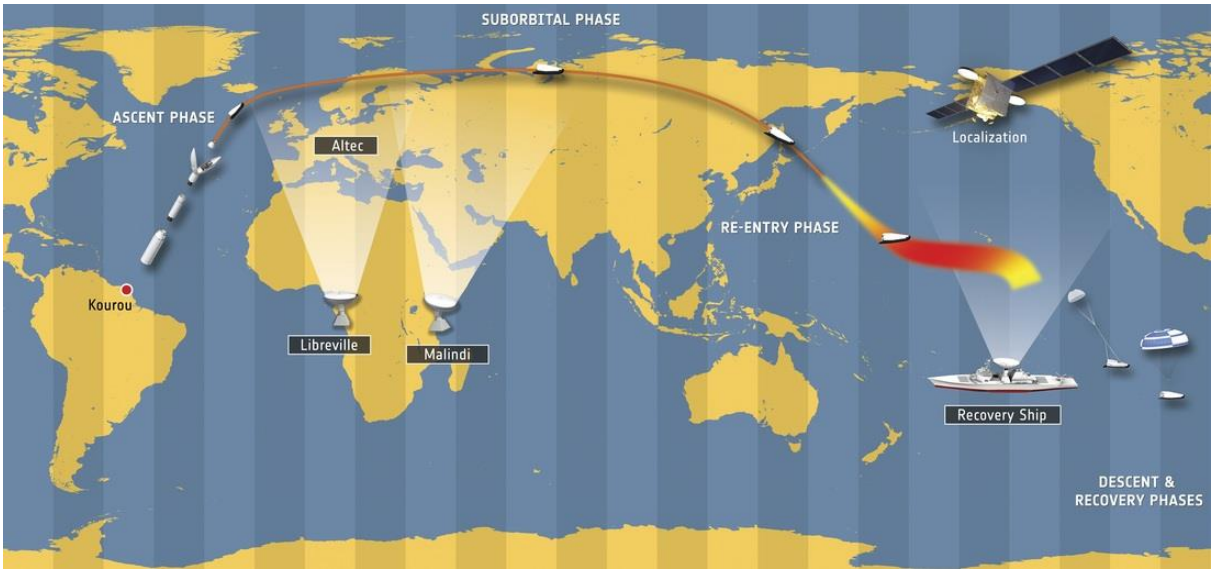

Figure 4: The IXV mission concept (credits: ESA)

3. IXV Flight Reconstruction

The IXV flight reconstruction consisted of a three steps process: (1) trajectory reconstruction from available sensors data, (2) flap deflection reconstruction, and (3) reconstruction of the moments acting on the vehicle during the flight.

3.1 Trajectory reconstruction

The adopted process of trajectory reconstruction involves the use of telemetry data from the IXV sensors completed by IXV initial conditions, aerodynamics configuration, atmospheric, wind and main body environment. The main navigation sensors are the IMU/INS (Inertial Navigation System) and the GPS. INS and GPS telemetry data stored at the OBSW level have been used in a coupled approach, making use of an Extended Kalman Filter (EKF) data fusion (see Figure 5), to fully reconstruct the inertial position, velocity, and the attitude state of the IXV from the lift-off until the splashdown.
From the reconstruction of the inertial position, velocity and attitude, it was possible to derive air-related parameters as the angle of attack (AoA), sideslip (AoS), airspeed, dynamic pressure, etc. as well as vehicle state in spherical coordinates (latitude, longitude, radius, relative velocity modulus, flight path and heading angles). The end-2-end altitude profile of the IXV flight is shown in Figure 6, as function of the time from lift-off. The main mission events are also reported. 1130 s after lift-off, the IXV separated from the VEGA AVUM stage to begin its orbital phase. About 220 s after separation, the IXV received the first GPS update, which was deemed not reliable due to the small number of satellites (only 4) used to produce the PVT solution, whereas the second GPS update was received almost 6 min later. From this moment on, the GPS was always available until blackout.

DOI: 10.13009/EUCASS2019-630

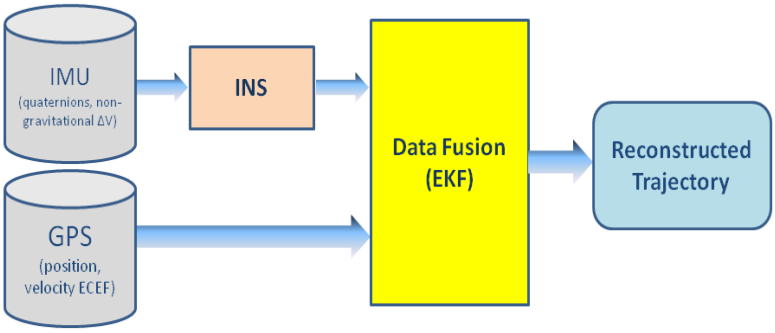

Figure 5: Trajectory reconstruction process

The reconstructed trajectory benefits from the availability of the GPS signal after the first GPS update, occurred 1348 s after lift-off, which on the contrary was not used by the IXV Navigation, that after accepting the first inaccurate GPS measurement labelled as valid, delayed the acceptance of the following correct measurement. This can be seen in Figure 7 (left), where the trajectory reconstructed deviates from the correct path at the first GPS update but then it gets back through the following updates. The O/B estimation stays on the incorrect path due to the first GPS update until it accepts its second GPS update only 270 s later.

IXV reached the Entry Interface Point at 120 km at about 3900 s after lift-off. During the Entry the IXV experienced communication blackouts due to plasma ionization and the formation of an envelope of ionized air around the vehicle, created by the heat from the compression of the atmosphere by the spacecraft. The ionized air interferes with radio signals, blocking any communication to and from the vehicle. In particular, the IXV during entry experienced two GPS blackouts, the first occurring at an altitude between 81 and 68 km, and the second one at an altitude between 67 and 62 km, with a consolidated reacquisition of the GPS signal starting from about 60 km. The effects of the second blackout can be seen in Figure 7 (right). During this second GPS blackout, the DDA filter of the IXV Navigation solution becomes active, estimating the altitude from the sensed drag. In this case the estimation of the altitude is evidently not correct as the estimated altitude (reported in green) deviates consistently from the correct path, showing an abrupt and not realistic increment of the altitude during the blackout estimated by the O/B solution. The reconstructed trajectory on the contrary corrects the solution making use of the available IMU measurements and improving the quality of the solution.

Eventually, at Mach estimated 1.5, at an altitude of about 25.4 km, the DRS is triggered and the descent sequence started. Finally, the vehicle splashed down in the Pacific Ocean about 5800 s (97 minutes) after lift-off.

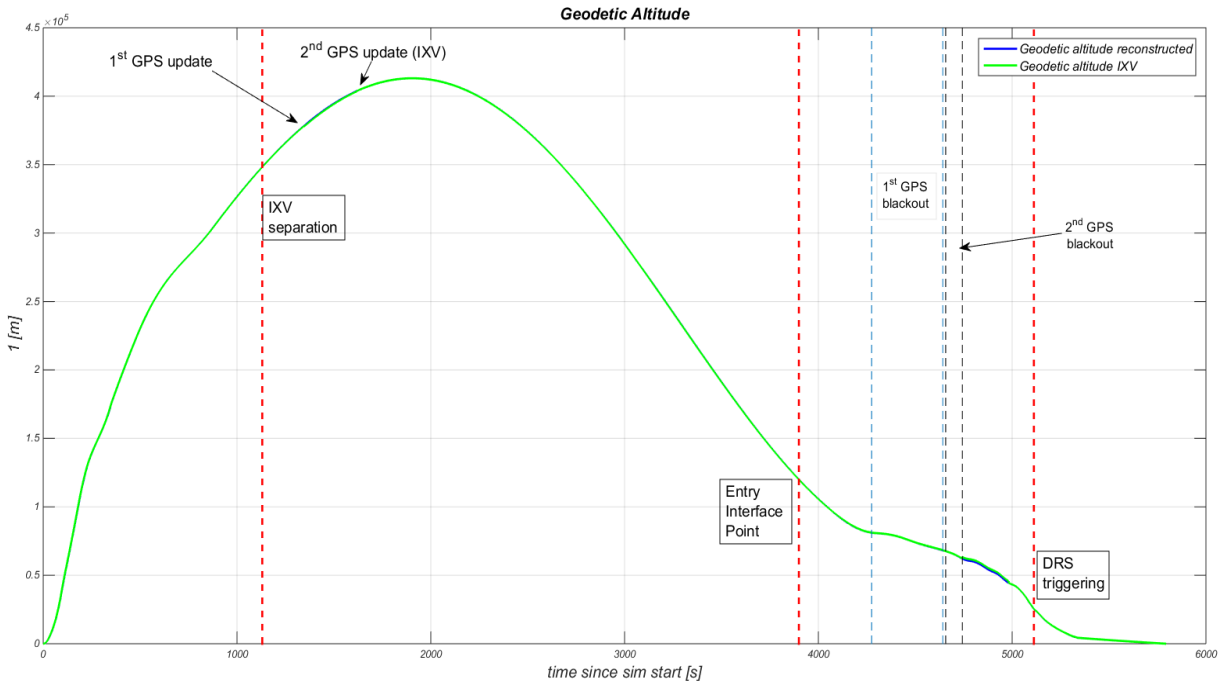

Figure 6: Geodetic altitude comparison between DEIMOS reconstructed trajectory and IXV navigation solution.

DOI: 10.13009/EUCASS2019-630

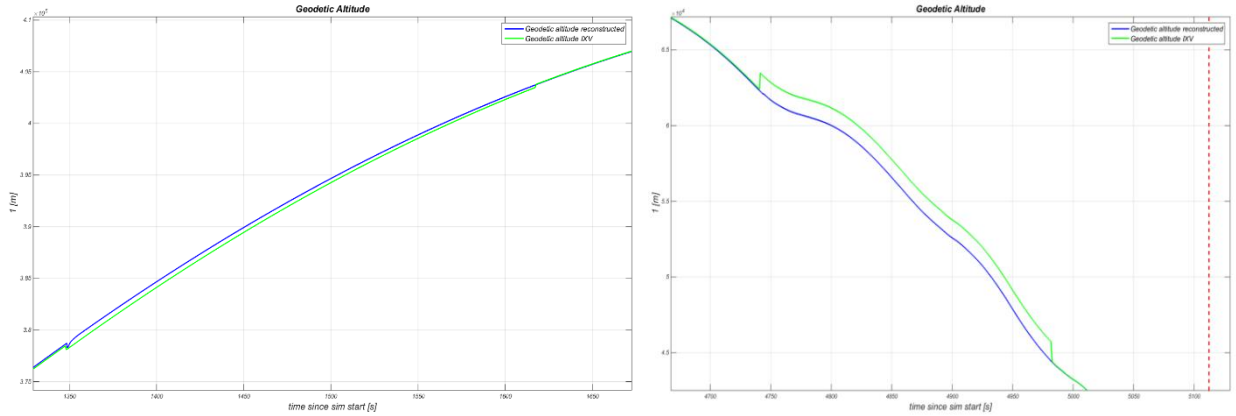

Figure 7: Reconstruction and O/B estimation of the trajectory once GPS measurements become available (left), GPS blackout during re-entry phase (right).

3.2 Flaps deflection reconstruction

No direct or indirect measurement (e.g. Infra-Red camera frames) of the actual deflection of the flaps was available to DEIMOS within the flight data, and only the deflections commanded by the GNC were directly available. For this reason, the reconstruction of the flaps' deflection had to be carried out with indirect methods, in particular filtering the commanded flap deflections with the model of the electro mechanical actuators. Additional inputs were taken from the reconstructed trajectory, and uncertainties in the flap model were considered as specified for the model.
With this approach, it was possible to define the envelope of the actual flaps' deflection. Figure 8 and Figure 9 provide for example the resulted left flap and elevon deflection variability as a function of time from the EIP. The 99% range variability envelope with 90% Confidence Intervals is reported, including the 50% percentile lines as well. The nominal flap model shot is also reported as a red line and the commanded flap deflection from the O/B telemetry is shown as a green line. The variability is contained within a band of approximately ±1 deg, providing a good estimation of what could have been the actual flap deflection during the flight.

3.3 Moments reconstruction

The moments experienced by IXV during its flight have been reconstructed making use of the angular rates from the telemetry, as estimated by the IMU, and the predicted Inertia of the vehicle from pre-flight measurements.
Figure 10 shows the reconstructed moments on X, Y and Z body axes with respect to the on-board telemetry time (OBET time) for the entry phase of the flight, from the EIP to the DRS triggering. On top of that, the reconstructed bank angle profile (amplified by a factor of 5) is shown in black and the reconstructed aileron profile (amplified by a factor of 200) is shown in grey. Selected events of the re-entry trajectory, in terms of altitude, dynamic pressure, or Mach number levels, are also reported as vertical black lines.
During the first part of the entry, between 85 and 120 km, the atmospheric density is low and the rarefied flow effects are dominant. The dynamic pressure is too low to guarantee an adequate effectiveness of the flaps, that are maintained at a pre-defined trim deflection. RCS is the only available actuator in this phase. The effects of the thrusters' firings are visible, mostly on My-Mz and partially on Mx, and become more intensive at the end of this phase, at an altitude of about 90 km, where high frequency oscillations on the pitch rate are observed (Figure 11). These RCS firings are commanded by the GNC to maintain the vehicle around the design trimline AoA of 45º while the natural tendency of the vehicle is to have a pitch down at first, above 105 km, to try to reach an aerodynamic trim at a lower AoA, and a pitch up afterwards, to try to reach an aerodynamic trim at higher AoA. An interval at which the vehicle reaches a trim is observed around 102 km of altitude, when the rate stabilizes briefly. This behavior disappears once the dynamic pressure rises and vehicle enters into the continuum flow regime, below 90 km, stabilizing its attitude around the designed aerodynamic trim position (AoA = 45º). From these results, and looking at the high frequency of the RCS actuation during this phase, seems that less fuel consumption could be achieved with an improved trim control strategy. The required GNC accuracy could be relaxed in rarefied flow, considering for example a control band within ±10º around the expected trimline vs the ±5º implemented in IXV. The impact on the aerodynamic performance of the vehicle shall be assessed, but it is expected to be minor. Moreover, alternative trim strategies could be evaluated, similarly to what proposed for the transonic flight of Space Rider (e.g. elevator trim approach, [10]). Smaller thrusters than those used in IXV could also help to reduce the control stiffness and the fuel consumption in this phase.

DOI: 10.13009/EUCASS2019-630

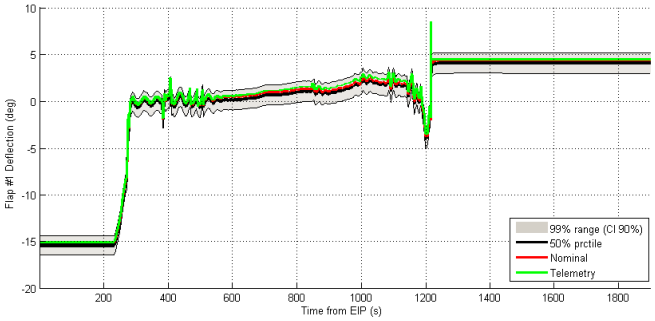

Figure 8: Reconstructed left flap deflection

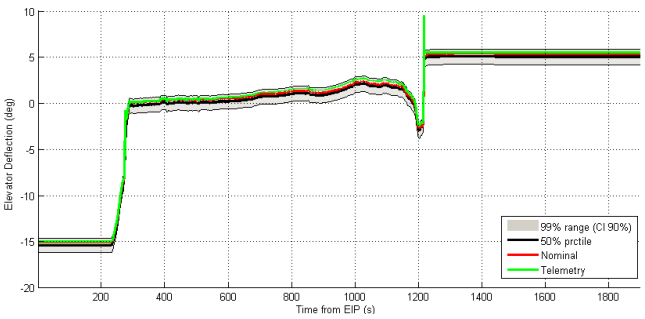

Figure 9: Reconstructed Elevon deflection

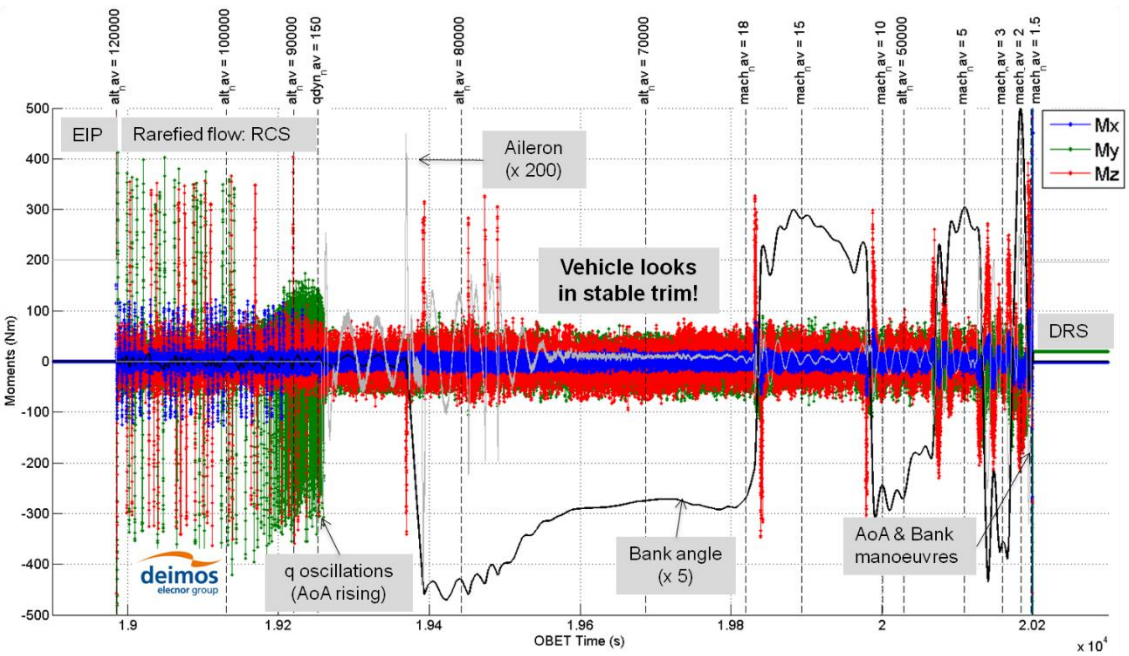

Figure 10: Reconstructed Moments (full entry phase)

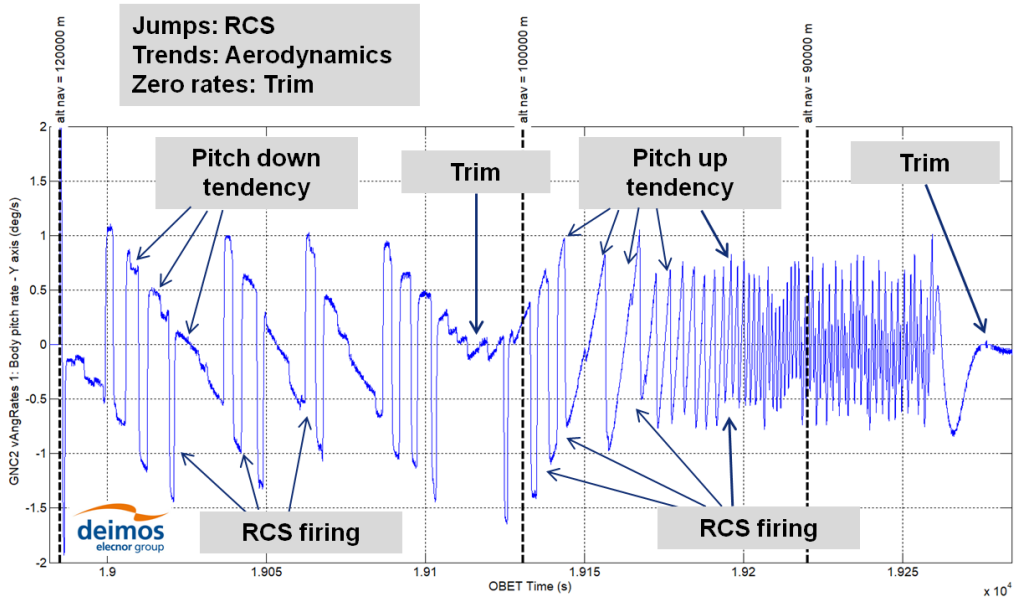

Figure 11: Aerodynamic trim tendency and RCS actuation in the rarefied flow

DOI: 10.13009/EUCASS2019-630

The analysis of the behavior in rarefied flow thus show that there is room for a consolidation of the trimline design and more in general of the trim control strategy in the rarefied flow, and should be considered for the Space Rider.
Below 90 km, the atmospheric density increases and the vehicle enters into the continuum flow. In the hypersonic phase, between Mach 25 and Mach 3, the vehicle appears generally to fly in a very stable trim condition, with limited total moments in the three axes. Peaks are observed in correspondence with bank maneuvers, performed through actuation of both RCS and aileron in order to control the AoS during the maneuver, and in particular when bank reversals are executed. The aileron deflection required decreases as the effectiveness of the flaps increases, in line with the increment of the dynamic pressure. This situation is maintained also in the supersonic phase, until Mach 2.5, when stronger actuations in pitch are visible due to the GNC commanding an increase in the AoA in order to follow the designed trimline for the supersonic phase. Moments are also smoother in this phase than in rarefied/hypersonic phases, where spikes were observed at the thrusters' firings. This indicates that the aerodynamic actuation, slower and smoother, was the dominant effect near the end of the entry flight, in line with what observed in [8].

4. IXV Flight Mechanics Post-Flight Analysis

With the trajectory and the main aerodynamic behavior reconstructed, the flight mechanics analysis of the IXV flight could be carried out. It is important in terms of analysis of the performance of the vehicle during the flight, and in order to validate and qualify the design and the design methodology with flight data, in order to confirm its applicability to future activities in general, and for the Space Rider program in particular.
The flying qualities (trim and stability) are key performances that were optimized during the design phase of the IXV program. A comparison of the design solution with the flight data shows that the flight data are generally within the design envelope during the full entry up to the DRS event, at about Mach 1.5, and close to the nominal values in most of the cases.
In terms of trim, the vehicle follows the designed trimline in hypersonic and supersonic, and the AoA maneuver commanded starting from Mach 2.5 is correctly followed (Figure 12), indicating also a very precise tracking performed by the GNC. At design level, a nominal 2.5 mm lateral offset of the IXV CoG_Y coordinate was taken into account, confirmed also for the flight predictions carried out right before the flight, while flight data indicate a null aileron deflection (Figure 12) and sideslip, which is an indicator of a potential symmetry of the CoG in XZ plane. Maneuvers in bank introduce transitory effects on trim, with the aileron punctually exceeding the range of static trim predictions envelope. This behavior was expected and observed in the design phase during the validation of the flight mechanics design with the results of the 6DoF GNC verification campaigns. In hypersonic the elevon is very close to the nominal value, with the exception of an interval between Mach 17 and Mach 5, where it is within the predicted range but about 1º lower than the nominal profile. A similar behavior is spotted in the supersonic phase, with the elevon between Mach 1.5 and Mach 2.5.

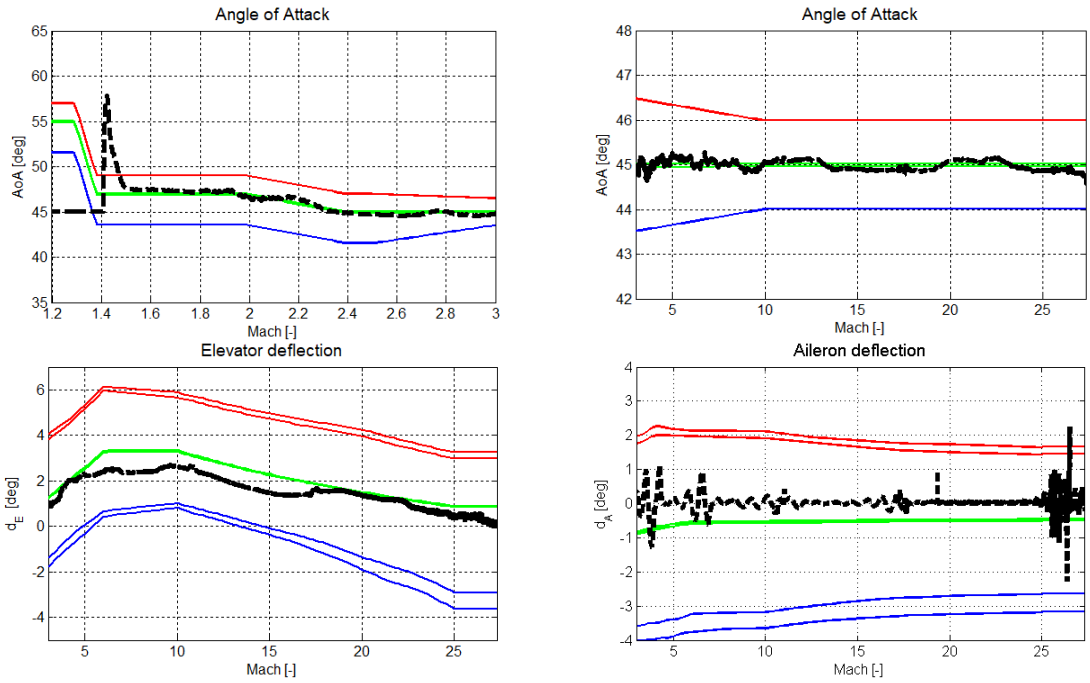

Figure 12: Comparison between predicted trim performance and flight trim performance

DOI: 10.13009/EUCASS2019-630

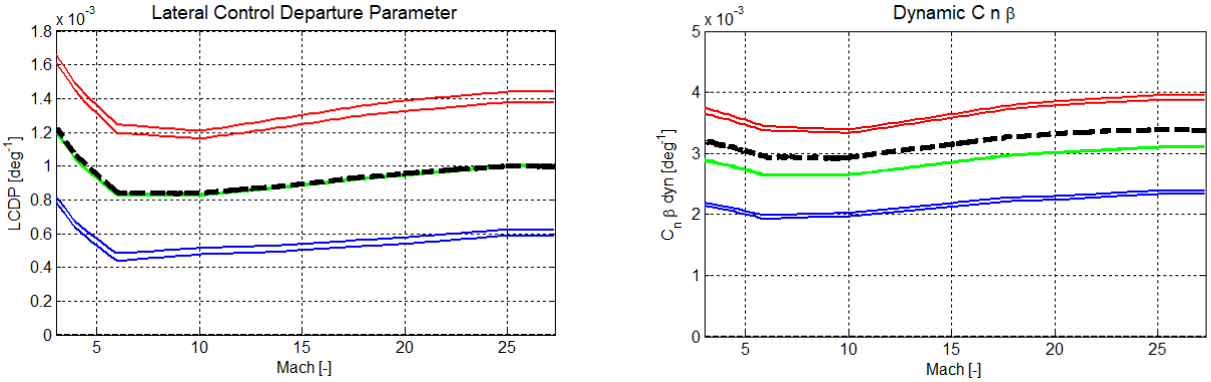

Figure 13 Flying Qualities comparison between predicted and telemetry data

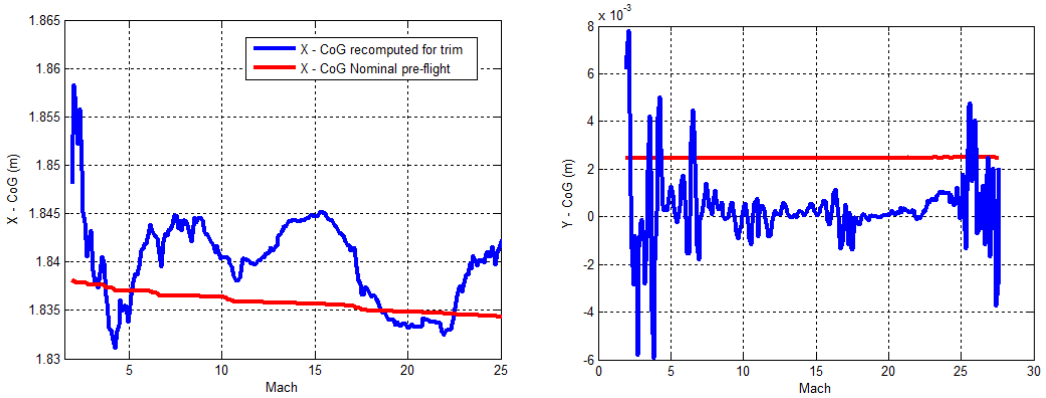

Figure 14: Comparison of the nominal CoG with the CoG required to trim the vehicle in the flight conditions reconstructed from the flight data

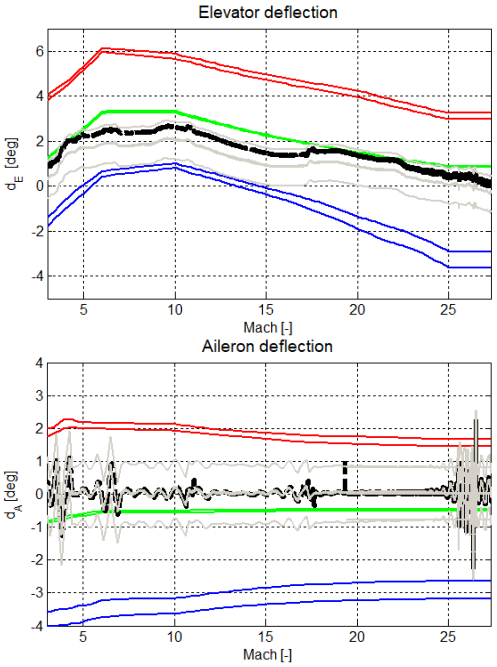

Figure 15: Elevon and aileron comparison between predicted and reconstructed data with uncertainties

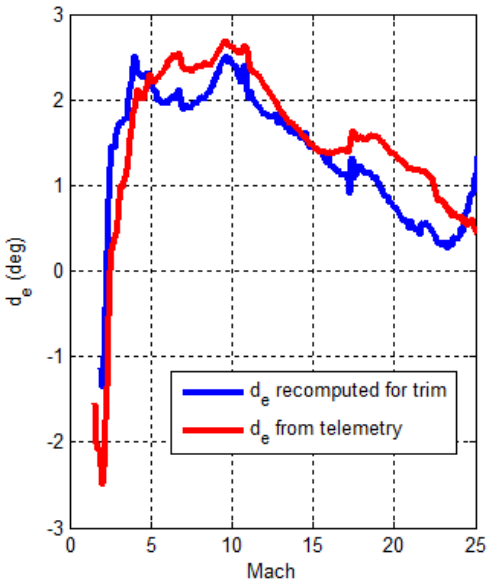

Figure 16: Comparison of reconstructed elevon deflection with the dE required to match the reconstructed aerodynamic forces

DOI: 10.13009/EUCASS2019-630

In terms of stability, the vehicle has been confirmed stable in hypersonic and supersonic, and with very good performance, longitudinally and laterally (Figure 13). No issues were observed, even when the RCS performance (important for the control of the AoS) were reduced or null, near the end of the Entry. The reconstructed Short period damping is a bit lower and out of predicted envelope for Mach > 5, while it is close to the nominal predicted value in the low hypersonic and supersonic phase. However, this parameter is highly influenced by the dynamic pressure and by the Inertia, and small imprecisions could have a large effect on the reconstructed flying quality. Similarly, the dynamic $C_N\beta$ is slightly biased with respect to prediction results. On the contrary, the LCDP is very close to the nominal prediction.
In general, the flight data showed that the IXV performed a re-entry flight in terms of flight mechanics parameters fully within the predicted conditions, and within the design conditions for which it was qualified, close to the nominal for the majority of the flying qualities. Moreover, tools and methodology used for the flight mechanics design and prediction provide the capability of correcting simulating the actual flight behavior.
The main significant deviation observed from the predicted nominal conditions (and yet, well within the predicted range) is the bias on the elevon deflection in hypersonic between Mach 17 and Mach 5, and in supersonic between Mach 2.5 and Mach 1.5. Such a behavior could be explained by an offset in the CoG_X or CoG_Z coordinates, a pitch moment coefficient higher than nominal, or a bias in the reconstructed AoA and elevon profile from the telemetry. For example, the CoG evolution during the entry flight was probably different from the nominal one due to the fact that the fuel consumption was higher than expected [6]. In particular, while the MIB during the orbital phase was expected to be close to 12Ns, its in-flight average during the orbital phase was approximately 34Ns [8], consistent with the increase in the fuel consumption and the increased number of firings. Nevertheless, the most likely explanation could be a combination of these different effects. Several tests were carried out with the objective of verifying the different contributions that could have resulted in the biased elevon deflection observed.
At first, a possible shift of the CoG was computed, and, making use of the reference IXV AEDB model, the moments required to trim the vehicle at the reconstructed AoA, AoS, and elevon/aileron deflections were computed. The results indicated that the pitch moment aerodynamic performance could have been higher than the nominal values. A similar test also confirmed that the CoG needed to trim the vehicle (in blue in Figure 14) was close to the pre-flight nominal (in red in Figure 14), but slightly forward, and symmetrical along the Y body axis.
On the other side, an alternative computation of the aerodynamic angles and the flap deflections was carried out, to compute the profiles needed to match the aerodynamic forces reconstructed from the IMU sensed accelerations. Results confirmed that a possible small bias in the reconstructed aerodynamic angles could exist, as well as a difference is noted between the nominal reconstructed elevon, and the recomputed one (see Figure 16). It is noticed in particular that the observed difference could partially explain the deviations between Mach 5 and Mach 20 observed in Figure 12, that on the contrary cannot be explained only with the uncertainty associated to the original flap reconstruction due to the flap model itself (see Figure 15, where the variability of the elevon profile associated to the flap reconstruction as explained in section 3.2 is reported in light grey, and compared with the FQ pre-flight predictions for both hypersonic and supersonic flight; it can be pointed out that there are still differences between the reconstructed profiles, including uncertainties, and the FQ pre-flight predictions).
Overall, the tests carried out confirmed that a combination of different factors likely concurred to be the reason for the elevon bias observed. All these conditions are anyhow very close to the nominal behavior and well within the expected envelope computed at design level, confirming the validity of the tools and methodology used for the flight mechanics design of the IXV.

5. IXV Mission Analysis Post-Flight

With the trajectory and the main aerodynamic behavior reconstructed, the mission analysis of the IXV flight could be carried out. It is important in terms of analysis of the trajectory performance of the vehicle during the flight, and in order to validate and qualify the IXV mission design and the mission analysis design methodology with flight data, in order to confirm its applicability to future activities in general, and for the Space Rider program in particular.
In particular, this comparison has been carried out splitting up the IXV trajectory in the following four phases:

- Ascent phase: from VEGA lift-off to the AVUM/IXV separation;
- Orbital phase: from AVUM/IXV separation down to EIP;
- Entry phase: from EIP to DRS trigger;
- Descent phase: from DRS trigger down to splashdown.

For the ascent phase, a comparison of the reconstructed trajectory with several optimized solutions produced throughout the IXV program is carried out. DEIMOS supported the verification of the feasibility of the mission by providing an independent ascent trajectory design during the phase C of program.

DOI: 10.13009/EUCASS2019-630

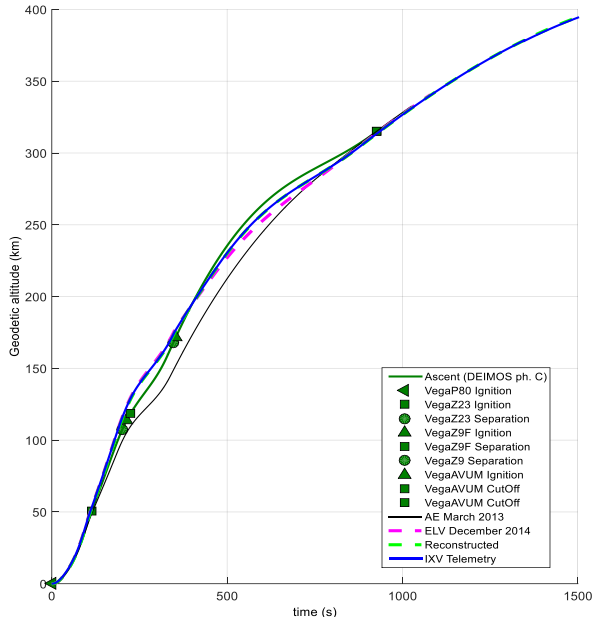

Figure 17: Altitude versus time during the ascent phase

Table 1: Orbital parameters at SEP

Data at Separation		Reconstructed		Pre-flight
Orbital parameters	**Units**	**value**	**sigma**	**NOM**
Semilatus rectum	km	6619.70	-0.13	6619.89
Eccentricity	-	0.026	0.00	0.026
Inclination	deg	5.44	0.97	5.43
RAAN	deg	244.96	0.24	244.90
Argument of periapsis	deg	-3.96	-0.71	-3.56
True anomaly	deg	128.02	0.71	124.80
Argument of latitude	deg	124.07	0.63	121.24
Semimajor axis	km	6624.09	-0.13	6624.28
Apocentre altitude	km	416.50	-0.09	416.71
Pericentre altitude	km	75.41	-0.13	75.59

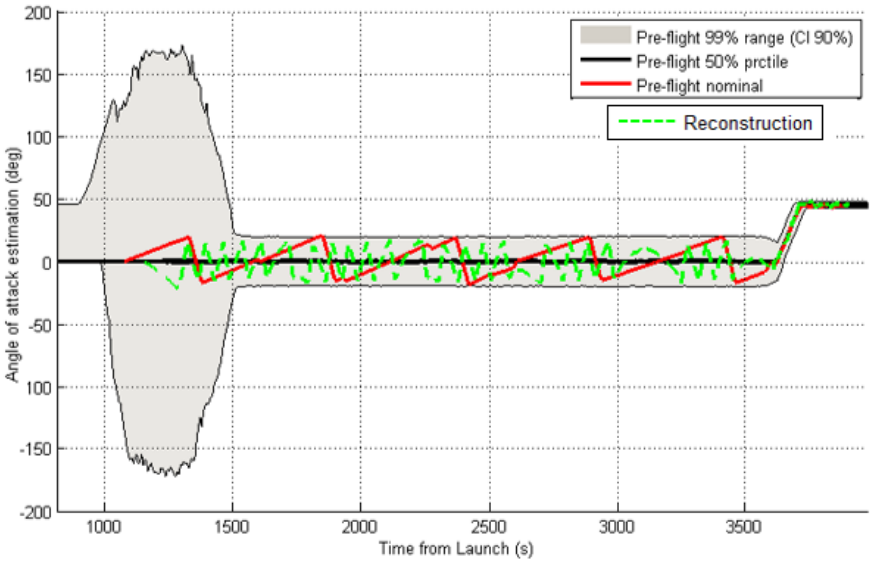

Figure 18: AoA during the orbital phase as function of time from Launch

Table 2: Corotating state parameters at EIP

Data at EIP		Reconstructed		Pre-flight
Corotating state	**Units**	**value**	**sigma**	**nominal**
Geodetic latitude	deg	-4.376	1.530	-4.484
Longitude	deg	174.764	1.295	173.390
Altitude above ground	km	120.000	0.000	120.000
Radius	km	6498.012	1.105	6498.007
Corotating velocity	km/s	7.438	3.054	7.435
Flight path angle	deg	-1.162	2.767	-1.211
Heading angle	deg	86.580	-1.180	86.695

DOI: 10.13009/EUCASS2019-630

Figure 17 shows the altitude versus time profile during the ascent phase of VEGA (from on-board telemetry and reconstructed) in comparison to the evolution of the optimized reference ascent trajectory during the IXV program. Despite differences are observed during intermediate phases of the ascent profile, the injection conditions show minimum deviations with respect to the phase C design, confirming the validity of the ascent trajectory design phase optimization performed by DEIMOS. Moreover, the reconstructed injection conditions showed that the performance of the launcher was close to the nominal, with a very high injection accuracy. All parameters are within 1σ with respect to the nominal pre-flight prediction (see Table 1). The injection was delayed in terms of time, with the IXV separating from the AVUM about 50 s later than predicted. This delayed separation led to the injection of IXV on the correct orbit but with a slightly different true anomaly (~3.3 deg).

The attitude at separation was close to nominal with a very low residual angular velocity. However, the effect of the over-actuation of the RCS can be observed in the faster than expected oscillations in the aerodynamic angles (see Figure 18, pre-flight results are shown in terms of 99% range variability with 90% Confidence Intervals, including the 50% percentile lines as well). In term of trajectory, this over-actuation in the orbital phase incremented considerably the residual delta-V in the direction of the X body axis, due to the 10 deg tilt angle of the thruster with respect to the YX-body plane, increasing the orbital energy at every actuation, and resulting in modified orbital parameters at the EIP. Due to this behaviour, the conditions at the Entry Interface Point are significantly different from the predicted one. In particular, the reconstructed trajectory shows a drift of about 150 km eastward at the EIP (see Figure 19), and shallower entry conditions (FPA and velocity at EIP around +3σ, see Table 2). In general, the IXV orbital flight occurred within the Monte Carlo variability of the pre-flight prediction, and therefore the IXV experienced in-flight conditions for which it was qualified.

During the entry trajectory, the Entry Guidance actuated to successfully compensate the high deviations at the EIP, and steered the vehicle to the nominal DRS location and conditions. The aerothermodynamic performance encountered by the vehicle were lower than those expected by the aero-thermo-dynamic database used for the design of the mission [9], therefore the margins with respect to the entry corridor were high. From Mach 2 to 1.5 the pre-release Guidance drove the vehicle to the DRS, following the correct trimline designed for the supersonic phase. The DRS was triggered when the estimated Mach reached 1.5 limit. The reconstructed trajectory showed that it occurred well within the DRS box, at an altitude of 25.4 km, and at less than 2 km from the nominal pre-flight prediction (Figure 20). Dynamic pressure, altitude and Mach are well within the predicted dispersion with margins with respect to the required DRS box. This result confirmed the validity of the flight prediction process, and in particular estimation of the correct wind conditions for the day of the flight, and the selection of the correct wind table to be used O/B by the GNC for the correct estimation of the Mach number.

Looking more in the details of the entry trajectory, the IXV performed an entry shallower than predicted, and therefore it flew the initial part of the entry, when the guidance is in open loop (during the first 400 s after the EIP) with a velocity and an altitude close to the maximum boundary of the flight prediction variability (see Figure 22 and Figure 23), consistent with EIP conditions close to 3σ values, and decelerating less than expected (Figure 24). At an altitude of about 80 km the dynamic pressure started to rise, and the Guidance switched to closed loop mode, about 1 min later than predicted. Starting from this point, the vehicle handles this excess of energy with a bank profile more aggressive than expected, which is needed to create enough drag to dissipate this extra energy and have almost zero vertical lift, from 400 to 800 s from the EIP, until an altitude of about 65 km. The actuation of the Guidance is therefore a response to the cumulated effects of a 150 km error at the EIP, and a shallower entry, resulting in a bank angle profile that in this time interval is outside the MC variability predicted pre-flight (e.g. first bank around 90 deg, see Figure 25). It was nevertheless within the qualification range of the IXV. After the first 800 s, the guidance command gets back within the predicted variability, confirming that the actuation in the initial part of the entry compensated the deviations observed, and the reconstructed trajectory is close to the nominal prediction. Between 800 and 1200 s the vehicle slowed down from 6 to less than 0.6 km/s, reaching Mach 2 at about 28 km. In this phase, the measured accelerations profiles are on average slightly higher than predicted. Most importantly, very large and very slow oscillations (below 0.01 Hz, Figure 24) are observed and were not expected. The entry trajectory is inside the entry corridor (Figure 26), but the drag and lift accelerations are different from the prediction, due to the high oscillations. The reason for these waves should be further investigated, to determine the source of such an unexpected behavior in the entry phase, and the impact it may have in Space Rider.

In the descent phase, the reconstructed trajectory showed a generally good matching with the pre-flight predictions. The duration was shorter than predicted (about 680 s), close to the lower bound of the predicted variability, and a higher than predicted velocity is observed below 5 km of altitude, during the descent under the main parachute. This behavior is compatible with a higher ballistic coefficient of the system under the main parachute, and therefore a lower drag.

The splashdown occured at about 5 km from the reference target defined at design level, but at about 1.5 km from the splashdown location predicted right before flight (Figure 21), with a splashdown velocity around 9 m/s. It is noted how all the predictions computed with the latest wind estimations are shifted toward the East with respect the reference design, performed with the design wind model.

DOI: 10.13009/EUCASS2019-630

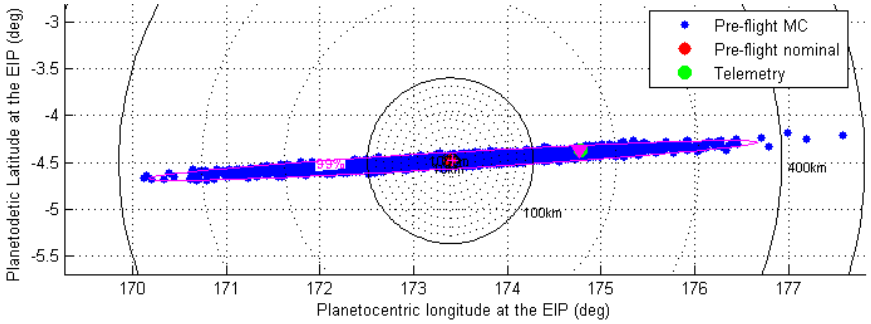

Figure 19: Reconstructed position at the EIP (magenta triangle) with respect to the predicted variability

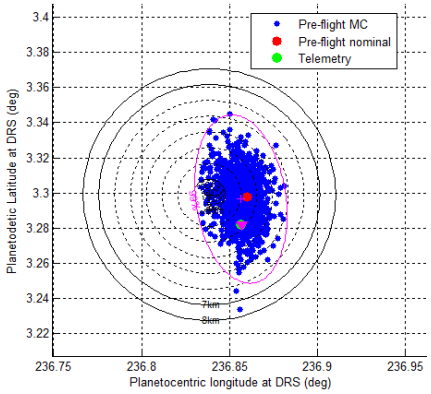

Figure 20: Reconstructed position at the DRS (magenta triangle) with respect to the predicted variability

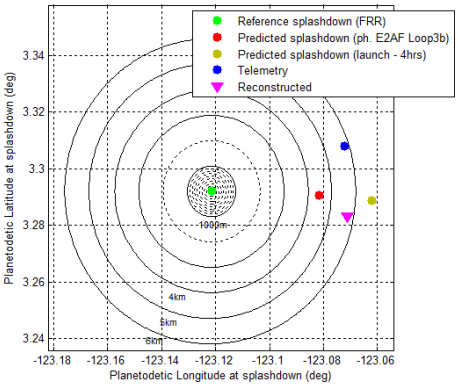

Figure 21: Reconstructed position at splashdown with respect to the different pre-flight predictions

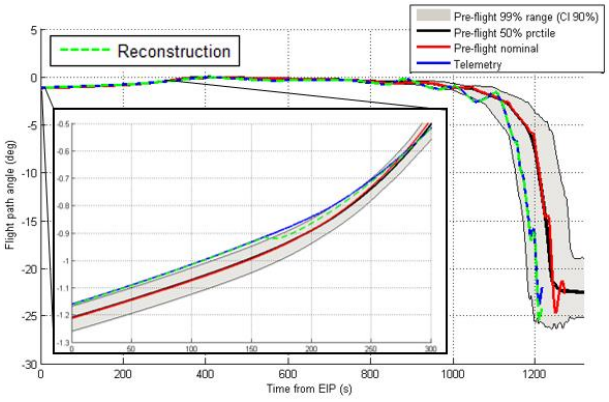

Figure 22: FPA during entry

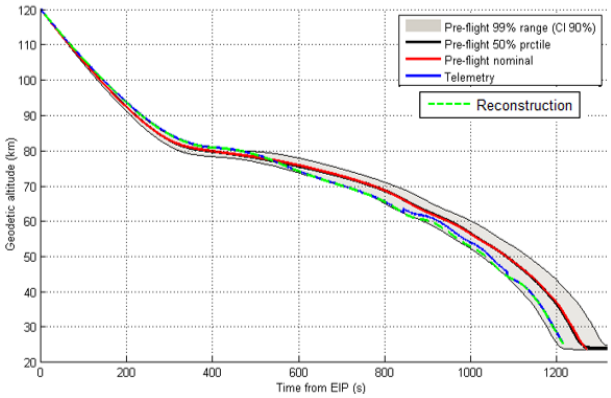

Figure 23: Geodetic altitude during entry

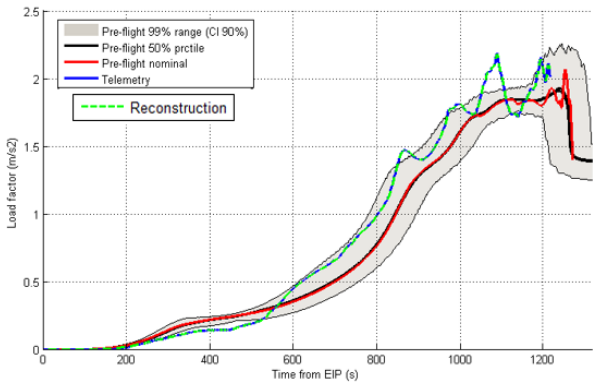

Figure 24: Total load factor during entry

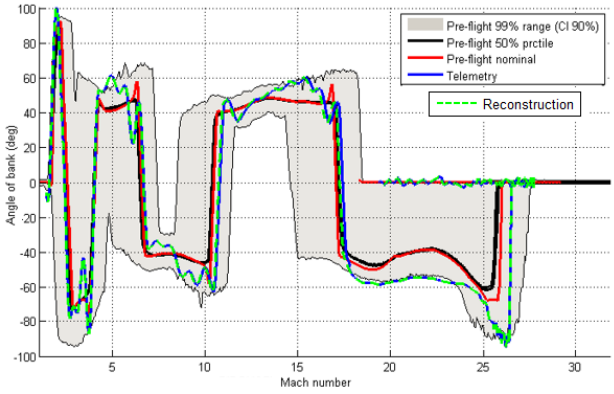

Figure 25: Bank angle during entry

DOI: 10.13009/EUCASS2019-630

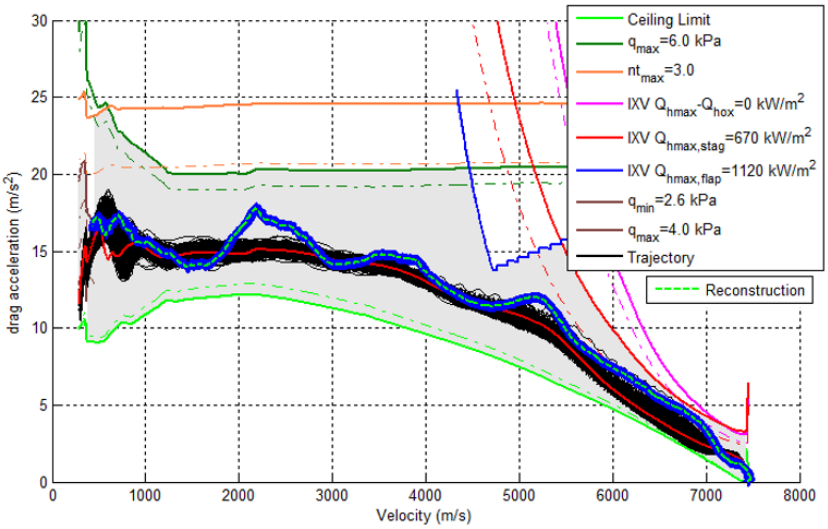

Figure 26: Reconstructed drag acceleration with respect to the Entry Corridor

6. Post-flight Prediction

As a final step of the post-flight analysis, a post-flight prediction was carried out, focusing on the re-entry phase. The objective is to compare the reconstructed flight performance during entry with the post-flight prediction made making use of the best estimation of data from the flight. The reconstructed conditions from the flight (EIP conditions from Table 2, as well as environment) have been injected in the 3DoF simulator used to carry out the pre-flight predictions [4][11], and the post-flight predicted entry trajectory was simulated. The results show that the post-flight predicted trajectory is very close to the reconstructed flight. In particular the bank angle is very close to the reconstructed profile, and the bank reversals occur with errors with respect to the reconstructed flight of a few seconds. The most relevant differences are during the first bank maneuver, right after the Entry Guidance switches to the closed-loop mode, but the post-flight prediction is very close to the reconstructed flight profile (see Figure 28). The post-flight prediction correctly replicates the shallow entry, and the increased drag during the hypersonic phase (see Figure 27). On the contrary, the post-flight prediction profiles do not have the low frequency oscillations observed during the last part of the entry, and discussed in the previous section of this paper (see Figure 27). This result further confirms the necessity of a detailed investigation at GNC level about this behavior, to determine the source of the oscillations, and assess the impact it may have in Space Rider.
Finally, these results further verify also the quality of the tools and the methodology used for the Mission Analysis of the IXV, flight-qualifying the Mission Engineering of the IXV.

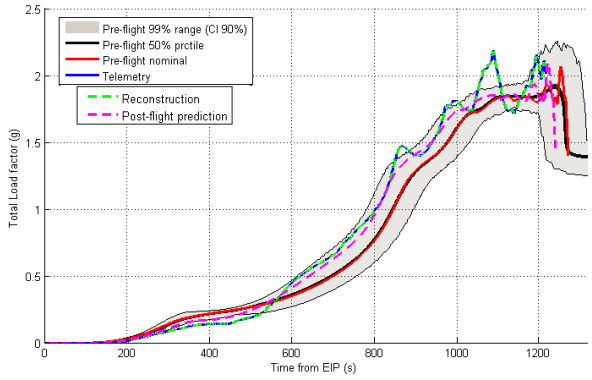

Figure 27: Total load factor during entry, post-flight prediction

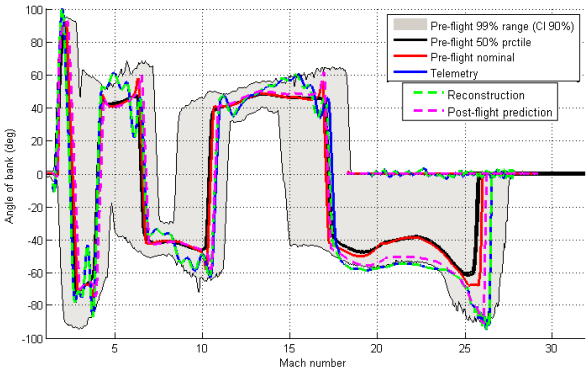

Figure 28: Bank angle during entry, post-flight prediction

7. Conclusions

The IXV program achieved a major success for Europe, when the IXV was flown successfully, completing its mission and achieving the objectives of the technology demonstrator. The reconstructed trajectory allowed analyzing the behavior of the IXV vehicle during the flight, Flight data are generally inside the predicted envelopes, and in many cases close to nominal values, verifying in general the pre-flight predictions performed by DEIMOS, and validating with flight data the Mission Engineering of the IXV, flight qualifying the design tools and design methodology in all phases of the flight. Therefore, the applicability of such methodology and tools for the design of the Space Rider mission is confirmed.
Lessons learned are derived from the post flight mission analysis, to be taken into account for the design of the Space Rider, as well as criticalities to be further investigated. A better characterization of the rarefied aerodynamics is recommended for the Space Rider, as well as a consolidation of the trim design and the trim control strategy in the same regime, that could reduce the GNC effort needed to control the vehicle in such conditions, and improve the fuel consumption. Smaller thrusters than in IXV could also help to reduce the control stiffness and the fuel consumption in this phase. During the entry phase the mission performance with respect to the entry mission goals and requirements were close to nominal: path constraints were within the limits, and the DRS events occurred close to the nominal prediction in terms of Mach, altitude, and position. The trajectory flown by the IXV vehicle was within the entry corridor limits, but some entry profiles were different from the nominal prediction, showing undesired oscillations that were not expected. It is recommended to further investigate the reason behind this behavior, to determine the source of such an unexpected performance in the entry phase, and the impact it may have in the Space Rider program.

Acknowledgments

The work has been performed under the Space Rider program in Phase B2 and funded by the European Space Agency. The authors wish to thank Thales Alenia Space Italia and ESA teams, for their support to the IXV and Space Rider mission analysis activities.

References

[1] Tumino G. et al. (2015) “The IXV Experience, from the Mission Conception to the Flight”, 6th EUCASS, Krakow, Poland.
[2] Denaro A. et al. (2015) “IXV re-entry demonstrator: mission overview, system challenges and flight reward”, 6th EUCASS, Krakow, Poland.
[3] Tran P. et al. (2007) “Re-entry Flight Experiments Lessons Learned – The Atmospheric Reentry Demonstrator ARD. In Flight Experiments for Hypersonic Vehicle Development”, Educational Notes RTO-EN-AVT-130, Paper 10, pp. 10-1 – 10-46, Neuilly-sur-Seine, France: RTO.
[4] Bonetti D. et al. (2015) “IXV Mission Analysis and Flight Mechanics: from Design to Postflight”, 23rd AIDAA, Turin, Italy.
[5] Bonetti D. et al. (2019) “Space Rider Mission Engineering”, 8th EUCASS, Madrid, Spain.
[6] Denaro, A. et al. (2015) “IXV Initial Post-flight Assessment”, 5th ARA Days, Arcachon, France.
[7] Sudars, M. et al. (2015) “IXV Trajectory Predictions and Flight Performance Overview”, 5th ARA Days, Arcachon, France.
[8] Kerr M. et al. (2017) “Flight performance of the IXV Re-entry Guidance, Control & DRS Triggering”, 10th ESA GNC Conference, Salzburg, Austria.
[9] Haya, R. et al. (2016) “IXV GNC Verification from Inspection to Flight Demonstration”, 6th ICATT, Darmstadt, Germany.
[10] Bonetti D. et al. (2018) "SPACE RIDER: Mission Analysis and Flight Mechanics of the Future European Reusable Space Transportation System", HiSSt Conference, Moscow, Russia.
[11] Bonetti D. et al (2016) "PETbox: Flight Qualified Tools for Atmospheric Flight", 6th ICATT, Darmstad, Germany.